ELECTRONICS AND ELECTRICAL ENGINEERING

ISSN 1392 – 1215 *2007. No. 7(79)*

ELEKTRONIKA IR ELEKTROTECHNIKA

ELECTRONICS

T170

ELEKTRONIKA

Spurious Fingerprint Minutiae Detection Based on Multiscale Directional Information

B. M. Popović, Lj. Mašković

Academy of Criminalistic and Police Studies,
Cara Dušana 196, 11080 Belgrade, Serbia, phone: +381 11 3161444, e-mail: cica@ptt.yu

M. V. Banđur

The Faculty of Technical Sciences, University of Priština,
Kneza Miloša 7, 38220 K. Mitrovica, Serbia, phone: +381 28 425320, e-mail: bandjo@ptt.yu

Introduction

Reliable and accurate automatic personal authentication is becoming a necessity for operation of modern society. Biometrics, as rapidly evolving technology which identifies people based on their physiological or behavioral characteristics, is becoming dominant over traditional means of authentication such as knowledge-based (something you know – password) and token-based (something you have – key) authentication. Biometrics has been widely used in forensics, and has the potential to be widely adopted in a very broad range of civil applications (ID cards, border control, physical access control, computer data security…). In another words, biometrics is becoming a necessary component of any ID management system. Amongst available biometric characteristics fingerprints are, due to their characteristics, one of the most researched, used and mature method of authentication [1, 2].

A fingerprint represents the image of the surface of the skin of a fingertip. A typical structure of a fingerprint consists of ridges and valleys.

The ridge pattern in a fingerprint can be described as an oriented texture pattern with fixed dominant spatial frequency and orientation in a local neighborhood. The frequency is depending on inter-ridge spacing, and orientation on flow pattern exhibited by the ridges. Region of a fingerprint where the ridge pattern makes it visually prominent are called *singularities* [3]. There are two types of fingerprint singularities: *core* and *delta*, and they are very useful for determining fingerprint's class.

A closer analysis of the fingerprint reveals some anomalies of the ridges, such as ridge endings, bifurcations, crossovers, short ridges, etc. These local features of fingerprints, called *minutiae*, can be used for manual or automatic fingerprint identification since their number and position defines fingerprint's individuality. The American National Standards Institute has proposed a classification of minutiae into four main groups: endings (terminations), bifurcations, crossovers and undetermined [4]. The most important ones are *ending* and *bifurcation*. Their discriminatory capability is very high. As shown in [5] the probability a fingerprint image containing 36 minutiae will match 12 minutiae with a different fingerprint also containing 36 minutiae is $6{,}1\times10^{-8}$ (i.e. is unique among 16 million fingerprints based on 12 corresponding minutiae pairs).

Typical structure and basic features of fingerprints (singularities and minutiae) are shown in Fig. 1.

Fig. 1. Basic features of fingerprints: ridge ending (in square), ridge bifurcation (in circle), core (X) and delta (in triangle)

Extensive research of automatic fingerprint identification system (AFIS), although started in the early 1960s, is still in focus of scientists around the world. A critical step for AFIS accuracy is reliable extraction of features (mostly minutiae) from the input fingerprint image.

There are a number of approaches for minutiae detection and a short overview can be found in [3]. Most of them includes following operations: preprocessing (segmentation and enhancement), binarization, thinning, minutiae extraction and post-processing [6,7,8,9], although some algorithms work directly on gray-scale image [10,11].

However, the effectiveness of a feature extraction relies heavily on the quality of the input fingerprint images. A number of factors (postnatal marks, occupational marks, characteristic of used acquisition device, etc) contribute to

fact that fingerprint images may not always have well-defined ridge structures, resulting in high number of spurious minutiae detection [12]. Consequently fingerprint image enhancement is usually the first step in most AFIS, and a minutia filtering (post processing) is necessary before matching algorithm is applied.

Various enhancement techniques for improving the clarity of the ridge structure in the fingerprint image have been suggested [9,12]. Since in local area, the ridges and valleys have well-defined frequency and orientation, it is natural to use directional filters in spatial [2] or frequency domain [12,13].

Although noise content is reduced, enhancement process can also introduce false ridges, resulting in false or missing minutiae. A number of minutiae filtering approaches have been presented, applied to binary [6,7,14,15] or gray-scale image [10,11], combining statistical and structural approach, using morphological filters or some other method for minutiae validation. But even high quality images can yield false minutiae, for example, when there are cuts and scars in fingerprint image.

In our work we were focusing on detecting and removing spurious minutiae in regions with broken ridges (often called creases). If those regions are large, enhancement techniques can not overcome spurious minutiae detection since ridges remains broken (in cases of small creases it is possible to reconnect ridges during enhancement process). Since most enhancement techniques use information about orientation fields, we tried to analyze if and how this information can be used in minutiae filtering algorithms. We extent our research [16] by including information about singular points position in our minutiae filtering algorithm.

Orientation field estimation

The ridge orientation in two dimensional space can be represented in two ways. First way is to represent the ridge orientation by a unit vector, forming angle θ with x-axis, as shown in Fig. 2a. The angle θ, called direction of the vector, is in the range $[0,2\pi)$. The alternative way is to treat the ridge as nonoriented line, as shown in Fig. 2b. In this case, the angle θ, is called orientation of the line and belongs to the range $[0,\pi)$. This second approach is more often useful in fingerprint analysis since it is difficult to determine the proper angle of unit vector in every pixel. However, in the literature dealing with fingerprint analysis, as well as in this paper, both terms "direction" and "orientation" are used as synonyms to denote ridge line orientation.

The first step in the analysis of ridge orientation is the formation of orientation (directional) image. This is a transformation of original fingerprint image into a matrix that represents local orientation of ridges in each pixel. It is used in fingerprint systems in different modules: enhancement, classification, ridge detection. There are a number of techniques that can be used to calculate orientation fields [2,17]. One common approach is the gradient-based method introduced in [18] and adopted by many researchers, see, e.g., [7,12].

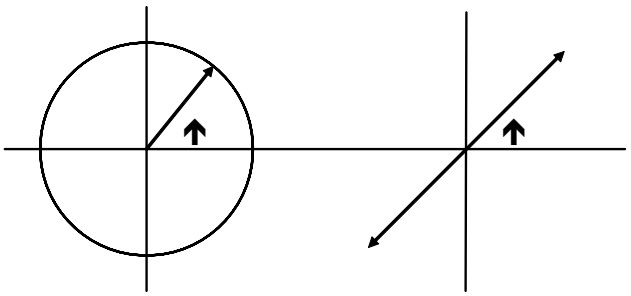

Fig. 2. Ridge orientation represented by: (a) vector, b) orientation

The elementary orientations in the image are given by the gradient vector $[G_x(x,y)G_y(x,y)]^T$, which is defined as:

$$\begin{bmatrix} G_x(x,y) \\ G_y(x,y) \end{bmatrix} = sign(G_x)\nabla I(x,y) = \\ = sign\left(\frac{\partial I(x,y)}{\partial y}\right)\begin{bmatrix} \frac{\partial I(x,y)}{\partial x} \\ \frac{\partial I(x,y)}{\partial y} \end{bmatrix}. \quad (1)$$

where $I(x,y)$ represents the original gray-scale image. Since opposite directions indicate equivalent orientations, the first element of the gradient vector has been chosen to always be positive. Since elements of directional fields are normal to the gradients in local area, one method of calculating the directional field for a given region is to set its direction (orientation) perpendicular to the average direction of its gradients [12]. Traditional solution of averaging squared gradients is used to avoid problems that are encountered when averaging gradients. The average squared gradient $[\overline{G_{s,x}}\ \overline{G_{s,y}}]^T$ can be calculated, in some neighborhood, using a possibly nonuniform window W as:

$$\begin{bmatrix} \overline{G_{s,x}} \\ \overline{G_{s,y}} \end{bmatrix} = \begin{bmatrix} \sum_W G_x^2 - G_y^2 \\ \sum_W 2G_xG_y \end{bmatrix}. \quad (2)$$

The average gradient direction Φ is given by:

$$\Phi = \frac{1}{2}\tan^{-1}\left(\frac{\sum_W 2G_xG_y}{\sum_W G_x^2 - G_y^2}\right), \quad (3)$$

where G_x and G_y are the horizontal and vertical components of the gradient at each pixel. Since the angle of gradient is perpendicular to the ridge orientation, the result obtained from (3) must be corrected for 90^0. Finally, the obtained dominant orientations are quantized to 16 possible values in the range [0, π]. We used Sobel gradient operator to obtain G_x and G_y, and the dimension of blocks we used for orientation estimation is $W = 8\times 8$.

As some pixels may have locally uncorrelated values, we may have a noisy version of the directional information. One of a commonly used approach is to split the image into blocks of size $W \times W$, and to replace each pixel of a block with the orientation exhibiting the highest frequency inside the block, forming so called block-directional image. Although this yield to abrupt direction changes from one block to another and requires additional smoothing, this block-directional image is useful for singular points extraction.

The singular points of fingerprint, *core* and *delta* can be found from the directional image using the Poincaré index [17]. The Poincaré index of a point in continuous two dimensional space is computed by summing up the changes in the direction angle around a small closed curve around the point, going in counter-clockwise direction:

$$P_{in}(x,y) = \lim_{\varepsilon \to 0} \frac{1}{2\pi} \int_0^{2\pi} \frac{\partial}{\partial \theta} D(x + \varepsilon \cos\theta, y + \varepsilon \sin\theta) d\theta, \quad (4)$$

where $D(x,y)$ is the average orientation at point (x,y).

The value of the Poincaré index is equal to 0 for an ordinary point, equal to ½ for a *core* singular point, and equal to -½ for a *delta* point.

In discrete two-dimensional space, the value of Poincaré index is computed in a closed curve, and integral in (4) is replaced by a sum. When computing the difference between two angles (which lies between -180° and 180°), the difference smaller in absolute value is taken. There can be maximum 4 singular points (2 cores and 2 deltas) extracted $\{S_k(x_k, y_k), where \quad k = 1,..,4\}$.

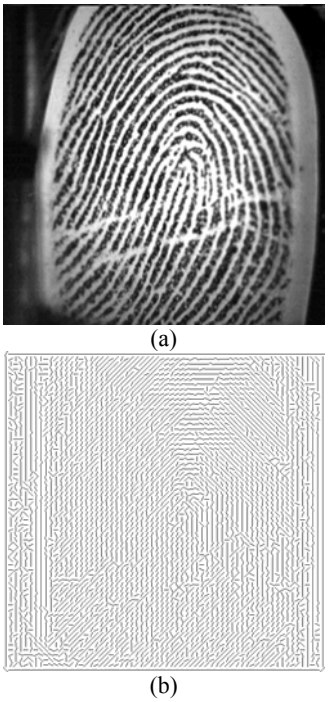

(a) (b)

Fig. 3. (a) Input fingerprint image, (b) orientation image

The final result of the algorithm for orientation field estimation, when applied to a fingerprint image is shown in Fig. 3. Notify that for convenience instead of presenting orientation in each pixel, we presented block-directional image.

Multiscale directional information estimation

Multiscale directional information is obtained by orientation field smoothing at a different scale.

In order to obtain finer directional information, instead of computing the block-directional image, we centered a block of size $W \times W$ at a given pixel, and attributed to it the highest direction frequency inside the block. We call that block as a smoothing window Ω.

Filtering (smoothing) the directional image by a smoothing window of different (increasing) size defines a multiscale representation of directional image with some useful information.

In our research multiscale directional information is obtained through two directional images D_s and D_l corresponding to the orientation image filtered with small Ω_s and large Ω_l smoothing window, where $s < l$.

Minutiae extraction

For minutiae extraction algorithm we use one presented in [8], whose modules (segmentation, enhancement, binarization, thinning and minutiae detection) will be briefly described.

Segmentation is basically dividing of image to regions with similar attributes. Background of fingerprint image is uniform with no useful information (all the important details – minutiae are to be found on ridges), and is useful to be excluded from further processing.

Since there is large variance of intensity in regions of ridges, opposite to uniform background, for segmentation we used variance calculation in block due to formula (5):

$$V(k) = \frac{1}{N} \sum \left[I_k(i,j) - M(k) \right]^2, \quad (5)$$

where $V(k)$ is variance for block k, $I_k(i,j)$ intensity in the pixel (i,j) of block k, $M(k)$ is mean of intensity for block k, and N is total number of pixels in block.

If the value of variance is greater from previously determined threshold T, block is considered to be in ridge region, else it is labeled as background and is excluded from further processing.

Enhancement is optional step and should it be used vary greatly from the quality of input image. When used, the enhanced image is expected to be more suitable than the original for visual examination and automatic feature extraction.

The Gabor filters are recognized as a very useful tool in computer vision and image processing applications. Gabor filters ere very useful both in frequency and spatial domain, due to their frequency-selective and orientation-selective properties. Properly tuned, Gabor filter can filter an image, maintaining only regions of a given frequency and orientation, and this has profound implications for research in fingerprint image analyze and enhancement using this filter.

An even symmetric Gabor filter general form in the spatial domain is described by formula [12]:

$$h(x,y,\phi,\omega) = e^{-0.5\{[x\cos\phi/\delta_x]^2+[y\sin\phi/\delta_y]^2\}}\cos(\omega x\cos\phi) \quad (6)$$

where ϕ – orientation of the Gabor filter, ω – frequency of sinusoidal wave along x axes, δ_x, δ_y – space constants of the Gaussian envelope along x and y axes, respectively. Fig. 4. shows an example of Gabor filter and its response in spatial and frequency domain.

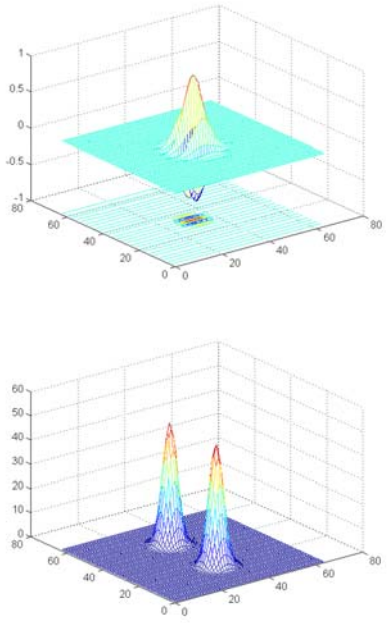

Fig. 4. The Gabor filter and its response in spatial and frequency domain

Parameters for optimal Gabor filter, ω, δ_x and δ_y, depend from average distance among ridges of fingerprint image. For our database and image of dimension 512×512 pixels, $\omega = 2\pi\ 60/512 = 0.736$ $\delta_x = \delta_y = 4$ is found to be optimal.

In our minutiae extraction algorithm applied method of enhancement is filtering input fingerprint image with bank of oriented Gabor filters (with 16 different orientations $\phi = i\pi/16$) in frequency domain [12].

For *binarization* process we apply LoG operator:

$$h_{LoG}(x,y) = \frac{1}{\pi\sigma^4}\left(1-\frac{x^2+y^2}{2\sigma^2}\right)e^{-\frac{x^2+y^2}{2\sigma^2}}. \quad (7)$$

We set threshold value to 127, and all pixels with value greater than threshold are set to active value 1, the rest are set to 0.

Thinning (skeletonization) of binary image is performed in order to simplify extraction of minutiae, since ridges obtained in previous step are a few pixels wide. We used line thinning by line following method [19]. As in case of ridge bifurcations it is possible that ridge remains wider from 1 pixel, as addition we apply classical OPTA or parallel thinning algorithms.

Minutiae detection is now trivial task by simply analyzing 3×3 neighborhood of pixel in following manner: let (x, y) denote a pixel in a thinned ridge, and N_0, N_1,…, N7 denote its 8 neighbors. Then:

- if $\sum_{i=0}^{7} N_i = 1$, pixel (x,y) is minutiae type ridge ending;
- if $\sum_{i=0}^{7} N_i = 3$, pixel (x,y) is minutiae type bifurcation;
- if $\sum_{i=0}^{7} N_i = 0$, pixel (x,y) is isolated and should be erased;
- if $\sum_{i=0}^{7} N_i = 2$, pixel (x,y) is on the ridge;

Imperfections in the input images will lead to undesired spikes and broken ridges in the fingerprint skeleton. They will create spurious minutiae, so the number of extracted minutiae can be an order of magnitude higher than the number of the true minutiae [6]. Some additional filtering (in order to remove short lines, connect endings and remove bifurcations at short distance) is necessary to eliminate false minutiae.

Minutiae filtering using multiscale directional information

Although enhancement by directional field can make some ridge breaks caused by narrow creases to connect, some broad creases remains. In the large regions of broken ridges (caused by scars and cuts), the detected orientation is significantly different (often perpendicular) from the actual ridge orientation. So the regions associated with the broken ridges are represented in orientation image by an abrupt change of orientation.

Knowing this we use multiscale directional information to estimate regions of broken ridges as follows [16]:

- Define two images D_s and D_l corresponding to the orientation image filtered with small (Ω_s) and large (Ω_l) smoothing window, where $s < l$;
- For given number of 16 discretised orientations, define the pixel (x,y) a member of set X that represent broken ridge region as follows:

$$(x,y) \in X, if\ \frac{5\pi}{16} \le |D_l(x,y) - D_s(x,y)| \le \frac{11\pi}{16}. \quad (8)$$

There is also, an abrupt change of orientation in regions where singular points (core and delta) exists. So it is possible, when applying rule (8), to detect those regions as false regions of broken ridges. In that case we may

falsely detect and filter genuine minutiae as spurious ones [16].

To overcome this problem we define minimum distance from singular points where crease can be found using rule (8) as $T_{\min}$. In that case all minutiae in the neighborhood of singular points are considered genuine.

Then we detect and filter spurious minutiae in following manner:

- We modify set X in a way that we exclude all pixels whose distance from estimated singular points $S_k(x_k, y_k)$ is less than $T_{\min}$;

$$(x, y) \notin X \quad if \quad dist(M, S_k) \le T_{\min} \tag{9}$$

where $dist(M, S_k) = \sqrt{(x - x_k)^2 + (y - y_k)^2}$

- We assume that every extracted minutiae M with coordinates (x, y) belonging to set X (obtained by (8) and (9)) is false;
- Since position of extracted minutiae can vary in a small range from the real one, we split the multiscale directional image to windows of size 8×8. Than for every pixel from set X belonging to a certain block, all pixels from the block are set to belong to set X. In that way all extracted minutiae with position inside those blocks are considered false.

Results

For our experiment we have set of 12 fingerprint images, where 11 are original 512 × 512 × 8bits containing some broken ridges, and 1 is modified in such a way that we added some white bars to create creases.

Smoothing window Ω used for obtaining multiscale directional information is set to size 15×15 for Ω_s, and size 39×39 for Ω_l. Minimum distance from singular points $T_{\min}$ is set to be 16.

Result of extraction regions of broken ridges for fingerprint 2(a) is shown in Fig. 5(a). Final result of minutiae extraction algorithm is shown on Fig. 5(b).

(a) (b)

Fig. 5. (a) Extracted regions of possible broken ridges; (b) Result of minutiae extraction algorithm (both for Fig. 2 (a))

Fingerprint we modified, in order to test our algorithm, is shown in Fig. 6(a). Extracted regions of possible broken ridges and final result of minutiae extraction algorithm are shown in Fig. 6(b) and 6(c) respectively.

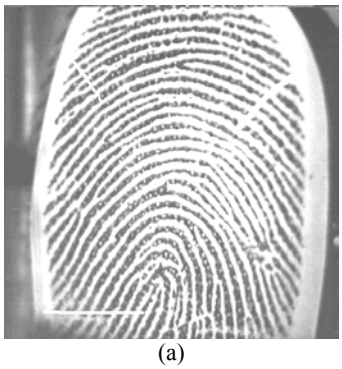

(a)

(b) (c)

Fig. 6. (a) Input modified fingerprint image; (b) Extracted regions of possible broken ridges; (c) Result of minutiae extraction algorithm

In order to compare effectiveness of presented method, we compared it with the method described in [8]. Results for two presented fingerprint images are shown in Table 1., where E represents number of minutiae determined by the expert; A is the number of automatically extracted minutiae; P is the number of matched (paired) minutiae; M is number of missing minutiae and F is the number of false minutiae

Table 1. Comparison of proposed method with minutiae extraction method presented in [8]

Fig. 2(a)	A	P	M	F	E
Method [8]	82	23	8	59	
Proposed method	56	21	10	37	31
Fig. 5(a)	A	P	M	F	E
Method [8]	93	23	7	70	
Proposed method	55	22	8	35	30

We can see that there is a significant decrease of number of false minutiae (for the whole set of tested images it varies from 30% to 55%). Although we lost some genuine minutiae (up to 15%), by using information about singular points position we manage to keep real minutiae that are in their neighborhood. Similar results were obtained for other tested images. Relatively high number of false minutiae is mostly result of binarization and thinning algorithms applied in minutiae extraction algorithm.

Conclusions

In this paper, we presented a method for spurious fingerprint minutiae detection. Although enhancement by directional filtering can reconnect some ridge breaks caused by narrow creases, some broad creases remain. Then multiscale directional information is used to detect and eliminate spurious minutiae in those fingerprint regions of broken ridges.

Characteristic results obtained by testing our algorithm on small database are shown, and some benefit in using presented method can be noticed. It will be a subject of further improving and testing on a larger fingerprint database. Our future work will be focused on improving minutiae detection algorithm in order to extract more genuine minutiae from the input fingerprint image.

References

1. **Federal Bureau of Investigation.** The Science of Fingerprints: Classification and Uses. – Washington, D.C. – U.S. Government Printing Office, 1984.
2. **Mehtre B. M.** Fingerprint image analysis for automatic identification // Machine Vision and Applications. – 1993. – Vol. 6. – P. 124–139.
3. **Yager N., Amin A.** Fingerprint verification based on minutiae features: A review // Pattern. Anal. Applic. – 2004. – Vol. 7. – P. 94–113.
4. **ANSI/NIST-CSL 1-1993,** Data Format for the Interchange of Fingerprint Information / American National Standards Institute, New York, 1993.
5. **Pankanti S., Prabhakar S., Jain A.** On the individuality of fingerprints // IEEE Trans Pattern Anal. Machine Intell. – 2002. – Vol. 24, No. 8. – P. 1010–1025.
6. **Farina A., Kovacs-Vajna Z. M., Leone A.** Fingerprint minutiae extraction from skeletonized binary images // Pattern Recognition. – 1999. – Vol. 32(5). – P. 877–889.
7. **Ratha N. K., Chen S., Jain A. K.** Adaptive flow orientation-based feature extraction in fingerprint images // Pattern Recognition. – 1995. – Vol. 28, No. 11. – P. 1657–1672.
8. **Popović B., Popović M.** Automatic fingerprint feature extraction for person identification // 3rd DOGS, Conference Proceedings. – Novi Sad, Yugoslavia, 2000.
9. **Jain A. K., Hong L., Pankanti S., Bolle R.** An Identity-Authentication System Using Fingerprints // Proc. IEEE 1997. – 85(9). – P. 1365–1388.
10. **Maio D., Maltoni D.** Neural network based minutiae filtering in fingerprints // Proc. ICPR, 1998. – No. 2. – P. 1654–1658.
11. **Jiang X., Yau W., Ser W.** Detecting the fingerprint minutiae by adaptive tracing the gray-level ridge // Pattern Recognition. – 2001. – Vol. 34, No. 5. – P. 999–1013.
12. **Hong L., Wan Y., Jain A. K.** Fingerprint image enhancement: Algorithm and performance evaluation // IEEE Tran. Pattern Ana. Machine Intel. – 1998. – Vol. 20, No. 8. – P. 777–789.
13. **Willis A., Myers L.** A cost-effective fingerprint recognition system for use with low-quality prints and damaged fingertips // Pattern Recognition. – 2001. – Vol. 34. – P. 255–270.
14. **Xiao Q., Raafat H.** Fingerprint Image Postprocessing: A Combined Statistical and Structural Approach // Pattern Recognition. – 1991. – Vol. 24, No. 10. – P. 985–992.
15. **Bhanu B., Boshra M., Tan X.** Logical templates for feature extraction in fingerprint images // Proc. Int. Conf. on Pattern Recognition(15th). – 2000. – Vol. 3. – P. 850–854.
16. **Popović B., Mašković Lj.** Fingerprint minutiae filtering based on multiscale directional information // Facta Universitatis(Nis), Series: Electronics and Energetics, Aug. 2007. – Vol. 20, No.2.
17. **Hong L., Jain A. K.** Classification of Fingerprint Images // In Proc. 11th Scandinavian Conf. Image Analysis, June 1999.
18. **Kass M., Witkin A.** Analyzing oriented patterns // Comput. Vision, Graph. Image Processing. – 1987. – Vol. 37, No. 4. – P. 362–385.
19. **Baruch O.** Line thinning by line following // Pattern Recognition Letters. – 1988. – Vol. 8. – P. 271–276.

Submitted for publication 2007 04 16

B. M. Popović, Lj. Mašković, M. V. Banđur. Spurious Fingerprint Minutiae Detection Based on Multiscale Directional Information // Electronics and Electrical Engineering. – Kaunas: Technologija, 2007. – No. 7(79). – P. 23–28.

Amongst available biometrics, personal identification based on fingerprints is still considered for one of the most reliable identification method. Most AFIS available today uses distinctive fingerprint features called minutiae for fingerprint comparison. Conventional feature extraction algorithm can produce a large number of spurious minutiae if fingerprint pattern contains large regions of broken ridges. This can drastically reduce the recognition rate in automatic fingerprint identification systems. In this paper multiscale directional information obtained from orientation image is used to detect and filter those spurious minutiae, resulting in multiple decrease of their number. Ill. 6, bibl. 19 (in English; summaries in English, Russian and Lithuanian).

Б. М. Попович, Л. Машкович, М. В. Бандур. Определение особенностей отпечатка пальца на основе мультимасштабной информации // Электроника и электротехника. – Каунас: Технология, 2007. – № 7(79). – С. 23–28.

Биометрическая идентификация, основанная на отпечатках пальцев, все еще является одним из самых надежных методов идентификации личности. Большинство сегодня доступных систем для сравнения отпечатков используют отличительные мелкие особенности отпечатка пальца. Обычный алгоритм извлечения особенностей может произвести большое количество ошибочных деталей, если образец отпечатка пальца содержит большие области прерывных линий. Это может значительно уменьшить надежность системы автоматической идентификации отпечатка пальца. В статье мультимасштабная направленная информация, полученная от ориентировочного изображения, используется, чтобы обнаружить и фильтровать ошибочные детали, приводя к многократному уменьшению их числа. Ил. 6, библ. 19 (на английском языке; рефераты на английском, русском и литовском яз.).

B. M. Popović, Lj. Mašković, M. V. Banđur. Smulkių pirštų atspaudų detalių aptikimas remiantis daugiapakope kryptine informacija // Elektronika ir elektrotechnika. – Kaunas: Technologija, 2007. – Nr. 7(79). – P. 23–28.

Biometrinė identifikacija pagal pirštų atspaudus vis dar yra laikoma vienu patikimiausių asmens tapatybės nustatymo metodų. Dauguma šiandieninių tokio tipo sistemų atspaudus palygina pagal smulkius išskirtinius jų elementus. Įprastiniai šių elementų aptikimo algoritmai dažnai duoda daug klaidingos informacijos, todėl gali labai pablogėti sistemos patikimumas. Šiems klaidingiems elementams aptikti ir filtruoti naudojama įvairių mastelių kryptinė informacija, gauta iš orientacinio vaizdo. Taip gerokai sumažinamas klaidingų elementų skaičius. Il. 6, bibl. 19 (anglų kalba; santraukos anglų rusų ir lietuvių k.).

DOI: 10.5755/j02.eie.10832